

Mobilities of O_2^+ and O_2^- ions in femtosecond laser filaments in air

Pavel Polynkin^{a)}

College of Optical Sciences, University of Arizona, Tucson, Arizona 85721, USA

(Received 22 August 2012; accepted 3 October 2012; published online 17 October 2012)

The operation of the capacitive plasma probe commonly used for measurements of plasma density in laser filaments and sparks in gases is analyzed. The probe is employed to measure absolute mobilities of O_2^+ and O_2^- ions produced through femtosecond laser filamentation in air. © 2012 American Institute of Physics. [<http://dx.doi.org/10.1063/1.4760280>]

Experiments on ionization of gases with short and intense laser pulses date back to the early 1960s. For over three decades, these experiments utilized Q-switched solid-state or gas lasers with pulse durations ranging from nanoseconds to microseconds and with Joule-level pulse energies. The mechanism of gas ionization with such lasers is through optically driven avalanche also known as optical breakdown.¹ More recently, another approach to gas ionization, through femtosecond laser filamentation, has been extensively investigated.^{2–4} Generally, avalanche ionization driven by nanosecond or longer laser pulses results in dense plasma plumes, but the length of these plasmas is limited by the Rayleigh length of the driving laser beam, typically in the region of few centimeters. Femtosecond laser filamentation produces extended plasma channels with the length of several meters and beyond, but plasma in these channels is dilute and very short lived. Very recently, a hybrid femtosecond-nanosecond approach has been suggested^{5,6} and experimentally demonstrated.⁷ Extended dilute plasma channels generated through filamentation of the femtosecond igniter pulse have been densified by the application of a co-propagating nanosecond heater pulse. This approach has been argued to combine the advantages of the straightforward control of plasma channel placement, offered by femtosecond laser filamentation, with the ability to create dense plasmas via optical breakdown.

Measurements of the basic parameters of laser-produced plasmas, whether generated through optically driven gas breakdown, femtosecond laser filamentation, or the hybrid femtosecond-nanosecond excitation, are not straightforward. The general problem with these measurements is related to the difficulty of accessing laser-generated plasmas directly. Three generic approaches to plasma diagnostic have been investigated and developed. One approach is based on the spectroscopic analysis of particular emission lines in the spectrum of fluorescence emitted by plasma.⁸ Another approach utilizes time-resolved interferometric techniques for the profiling of the spatial refractive index perturbations resulting from the presence of plasma.⁹ The third approach is based on electrostatic probing and/or charge collection. Generally, spectroscopic and interferometric techniques can be accurate and they can, in principle, yield quantitative information about laser-produced plasma. However, the implementation of these techniques is challenging. Spectroscopic characterization requires the resolution of narrow spectral lines in very

short time intervals characteristic of the plasma lifetime, often in the sub-nanosecond range. Interferometric techniques are based on complex pump-and-probe optical setups and sophisticated signal processing. Electrostatic and charge collection-based approaches are much simpler to implement, but they are indirect and rely on certain assumptions about the charge transport within the laser-generated plasmas. Generally, the electrostatic and charge-collection techniques can only yield information about plasma parameters on an arbitrary-unit scale.

The present letter is about one particular kind of diagnostic for plasma in laser filaments and sparks, based on the free-charge collection with a capacitive plasma probe. We will further restrict our consideration to femtosecond laser excitation. The probe considered here is schematically shown in the inset in Figure 1. It consists of two parallel electrodes connected to an external voltage source and placed on either sides of the laser-produced plasma channel. With no plasma present between the capacitor plates, there is no current flowing through the circuit, thus the voltage drop across resistor R equals zero. As plasma is created inside the capacitor through the application of the laser pulse, a transient voltage waveform $V(t)$ is generated and recorded. Amplitudes of various features in this waveform are used to quantify the peak plasma density, on an arbitrary unit scale.

The application of the above-described probe has been reported in the very first paper on optical gas breakdown with a Q-switched nanosecond laser.¹⁰ In that original publication, it was assumed that the probe collected all generated electrons and ions, an assumption that was not justified by any arguments. The use of a similar probe has been since reported in numerous papers on plasma generation with both nanosecond

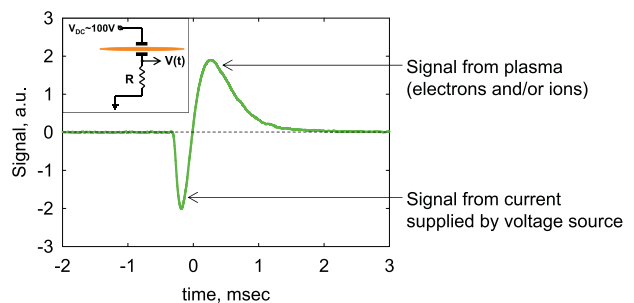


FIG. 1. Typical waveform measured with the capacitive plasma probe, after electronic low-pass filtering, e.g., with a bandwidth-limited oscilloscope. The inset shows the schematic of the probe.

^{a)}Electronic mail: ppolynkin@optics.arizona.edu.

and femtosecond lasers.^{7,11–13} Recently, an attempt to perform a single-point calibration of a probe of this type, using holography, has been reported.¹⁴

However, an uncertainty still exists about the nature of the signal returned by the kind of probe described above. Although the use of such a probe is frequently mentioned in the literature, the actual probe waveforms have not been published, and there is currently no widely accepted agreement on the polarity of these waveforms. In the present letter, we will analyze the principles governing the operation of the capacitive plasma probe. We will show that the typical probe waveform contains features resulting from different physical effects. We will argue that the features associated with the charge collection by the capacitor plates can be used to approximately quantify the variations in the peak plasma density, on an arbitrary unit scale, if the charge transport characteristics in the generated plasma are known and consistent from one experimental realization to another. At the same time, the signal feature due to the polarization of plasma inside the capacitive probe is relatively insensitive to the absolute value of plasma density. That feature can be used as an indicator of the existence of plasma, but it is a poor quantifier of the generated plasma density.

The generic shape of a typical waveform returned by the plasma probe is shown in Figure 1. The waveform comprises negative and positive swings of the signal. The appearance of the positive swing is relatively consistent with respect to the particular realizations of the probe setup. The peak value of this part of the signal is found to be linearly proportional to the bias electric field inside the capacitor, with a small threshold of the order of several tens of volts per centimeter. The appearance of the negative swing of the waveform depends on the proper grounding of the probe circuit and it is sensitive to the placement of dielectric objects in the vicinity of the setup. The peak value of the negative swing of the waveform grows with the bias electric field, but the dependence is not linear and starts to saturate at a bias electric field of several hundred volts per centimeter.

Let us identify various physical effects that contribute to the probe waveform. Before the appearance of the plasma channel between the capacitor plates, the capacitor is charged, and no current flows through the resistor R . Accordingly, the voltage drop across the resistor is zero. As plasma is created by an ultraintense laser pulse undergoing filamentation, the plasma channel quickly becomes polarized through the positive and negative components of plasma shifting with respect to each other in the external DC electric field of the probe. Consider the plasma channel as a cylinder with a diameter of $\sim 100\ \mu\text{m}$ and with charge density of $\sim 10^{16}/\text{cm}^3$, according to the recent interferometric measurement.⁹ Assume that the maximum polarization of this plasma results from the separation between the positively and negatively charged constituents of the channel by the distance at which the electric field, induced by the separation of the positive and negative components of the cylindrical channel, becomes equal and opposite to the external bias field. In that case, the maximum charge separation is directly proportional to the bias electric field and inversely proportional to the density of plasma in the channel. Since the dipole moment of the polarized channel is proportional to plasma density in the

channel times the charge separation, the maximum dipole moment turns out to be approximately independent on the density of plasma.

Given the above estimates for the plasma-channel diameter and plasma density, the separation between the positively and negatively charged components of the channel, at which the electrostatic attraction between them balances out the polarizing force from the external bias electric field $\sim 100\ \text{V}/\text{cm}$, is of the order of $1\ \text{\AA}$, which is much smaller than the estimated Debye length of plasma in the filament. The time interval it takes to separate the positive and negative charge constituents by a distance of that order is in the range of several hundred femtoseconds, which is too fast to be detected by electronic means. After the channel is polarized, free charges inside the capacitor plates will re-distribute so that the component of the net electric field near the capacitor plates is perpendicular to the plates. That charge re-distribution is equivalent to the appearance of image dipoles, shown schematically in Figure 2, as well as the images of those images, and so forth. The corresponding charge re-distribution will happen within the time interval of the order of the plate separation divided by the speed of light, which is of the order of several tens of picoseconds. That is still too fast to be detected electronically and to appreciably affect the appearance of the signal waveform. Further, the charge imbalance inside the capacitor will be compensated by the inflow of additional charges from the DC voltage source. Depending on the time constant of the circuit formed by the capacitor and the load resistor, that process will occur on the nanosecond to microsecond time scale, which can be electronically detected. The important consideration relevant to the present discussion is that the polarity of the corresponding swing of the probe waveform will be negative, and that the amplitude of the swing will be proportional to the peak dipole moment induced in the plasma channel by the external bias field. According to the above discussion, the peak dipole moment is approximately independent of the plasma density in the channel, thus the amplitude of the negative swing of the waveform is also independent of the plasma density.

Most of the electrons and ions within the laser-induced plasma channel will eventually recombine and not reach the electrodes of the plasma probe. However, a very small fraction of the charges that occupy the outer-most wings of the spatial charge distributions, as shown in Figure 2, will drift towards

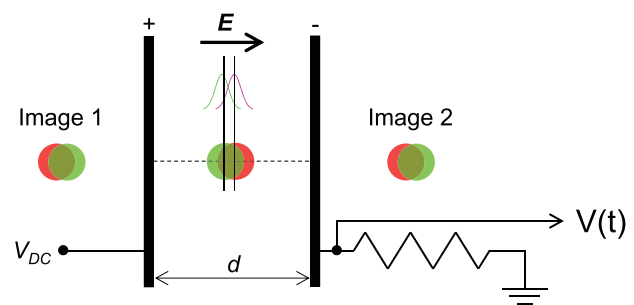


FIG. 2. Schematic of the capacitive plasma probe showing charge separation within the plasma channel and two electrical image dipoles on the either side of the capacitor plates.

the capacitor plates and contribute to the positive swing of the signal waveform. The electron mobility in atmospheric-pressure gases is in the range from 1 to $10 \text{ m}^2/\text{V} \cdot \text{s}$,¹⁵ while the ionic mobility is in the $\sim 10^{-4} \text{ m}^2/\text{V} \cdot \text{s}$ range.¹⁶ Accordingly, for a bias electric field of 100 V/m, electrons and ions will reach the corresponding electrodes of the plasma probe within microseconds and milliseconds, respectively. Both of those time scales are detectable electronically.

In air, electron attachment to neutral oxygen molecules, the process that occurs on the picosecond time scale, will prevent essentially all free electrons from reaching the positively charged plate of the plasma probe. In that case, the measured positive swing of the signal will be due to the singly charged positive and negative molecular oxygen ions reaching the negative and positive electrodes of the probe, respectively.¹³

As an example of the application of the capacitive plasma probe, consider the case of the plasma channel produced through filamentation of a sub-40 femtosecond laser pulse with 800 nm center wavelength and millijoule-level pulse energy. The laser beam, with a 1 cm diameter, is weakly focused by a mirror telescope with the effective focal length of 2 m. The plasma probe consists of two $1 \text{ cm}^2 \times 1 \text{ cm}^2$ square copper plates separated by a distance of 1 cm and charged to the bias voltage of 400 V. The results of the longitudinal profiling of the generated plasma are shown in Figure 3, at different levels of peak power of the laser pulse. Each data point shown has been averaged over 100 laser shots. In the top panel, the peak power of the pulse is 7 GW,

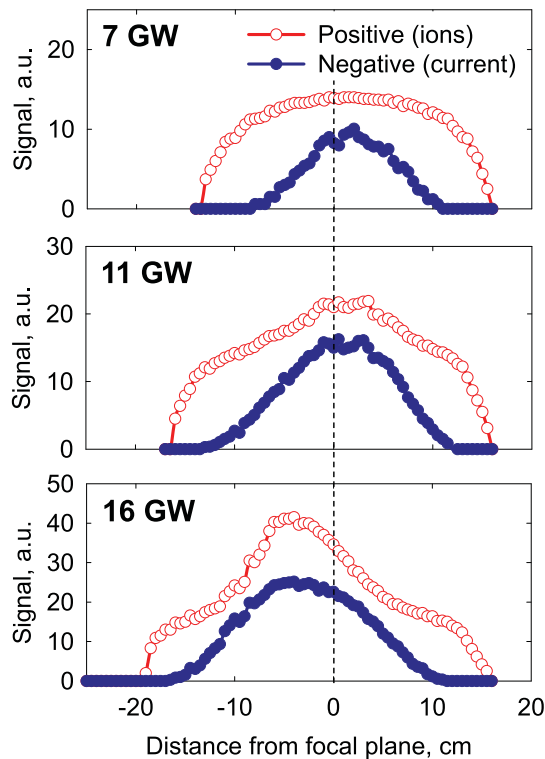


FIG. 3. Profiling of plasma in a femtosecond laser filament created in air by weakly focused femtosecond laser beam, for three values of the peak laser power. The amplitude of the positive swing of the probe waveform develops a bump feature in the vicinity of the focal plane, when the peak power exceeds the critical power for self-focusing. The amplitude of the negative swing of the signal remains feature-less.

which is below the critical power for self-focusing of the laser beam. Nevertheless, some plasma is generated through the multi-photon ionization process, as the on-axis intensity of the beam in the vicinity of the focal plane of the telescope is made high enough by the external focusing. The plots of the peak values of both the negative swing of the probe waveform, resulting from the transient current, and of the positive swing due to ions reaching the capacitor plates, vs. distance, are feature-less bell-shaped curves. As the input peak power of the laser pulse is increased above the critical power for self-focusing collapse (middle and bottom panels in Figure 3), the positive part of the signal develops a bump near the focal plane of the weakly focused laser beam. The negative part remains feature-less. The bump in the ionic signal is indicative of the enhanced plasma production due to the on-set of high on-axis intensity that accompanies the self-focusing collapse of the beam. The ionic feature of the signal captures the collapse event, but the feature with the negative polarity, which is due to the transient current, does not. The length of the filament deduced from the visual observation of the faint fluorescence emitted by the plasma approximately coincides with that of the bump feature in the ionic signal measured by the probe.

If the entire capacitive probe is shifted sideways with respect to the plasma channel, while keeping the distance between the plates and the bias voltage constant, positive or negative ions will have to travel further before reaching the corresponding plate of the probe, depending on the sign of the shift Δx . Accordingly, the positive peak of the waveform will split into two sub-peaks, as shown in Figure 4. The delay of the lagging sub-peak will increase as the transverse shift of the probe increases. This observation allows one to directly measure the mobility of ions produced inside the plasma channel. To conduct such a measurement, the probe was shifted transversely, bringing the positive or negative electrode closer to the plasma channel. For the case of plasma produced through femtosecond laser filamentation in air, the part of the waveform that corresponds to the positive or negative molecular oxygen ions, depending on the direction of the shift of the probe, splits off from the waveform and becomes readily identifiable. The drift velocity for the ions responsible for the split-off peak is calculated by dividing the distance between the plasma channel and the further

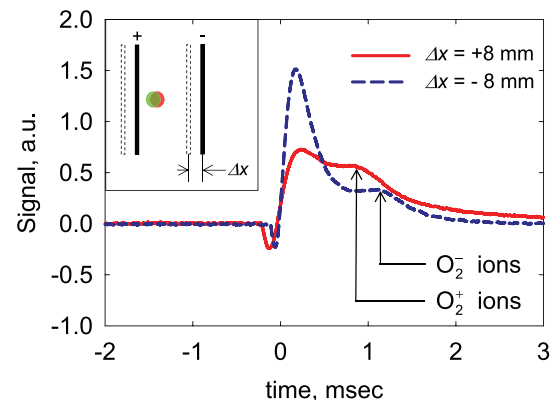


FIG. 4. Signal waveforms for the cases of the plasma channel positioned closer to positively or negatively charged capacitor plate. The lagging peaks in the waveforms are due to positive and negative oxygen ions.

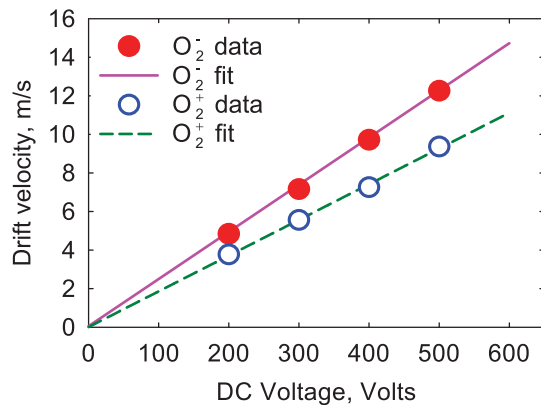


FIG. 5. Drift velocities of the O_2^+ and O_2^- ions in air vs. bias voltage.

electrode by the time delay corresponding to the position of the lagging peak on the waveform. Keeping the position of the plasma probe fixed, we increase the bias electric field applied to the probe and plot the drift velocity vs. bias field. The resulting curves, for the case of a laser filament in air, are shown in Figure 5, for positive and negative transverse shifts of the probe. The dependence of the drift velocity on the bias electric field is linear for both positive O_2^+ and negative O_2^- molecular ions, as expected. The slope of these lines equals the mobilities of the corresponding ions. By calculating the slopes, we find, for the mobility of positive and negative molecular oxygen ions in air, under normal conditions, values of $1.8 \times 10^{-4} \text{ m}^2/\text{V} \cdot \text{s}$ and $2.4 \times 10^{-4} \text{ m}^2/\text{V} \cdot \text{s}$, respectively. These values are close but not equal to the previously measured mobilities of the positive and negative molecular oxygen ions in pure oxygen gas, under normal conditions, which have been found to equal $2.2 \times 10^{-4} \text{ m}^2/\text{V} \cdot \text{s}$ and $3.3 \times 10^{-4} \text{ m}^2/\text{V} \cdot \text{s}$, respectively.¹⁶ Using femtosecond filamentation for the excitation of ions within a mixture of gases, such as air, allows for the selective ionization of a particular constituent of the gas that has the lowest ionization potential. That way the mobility of specific ions in a gas mixture can be quantified. This is a unique capability offered by femtosecond laser filament excitation, which is not readily accessible by alternative means of ionization.

In conclusion, we have analyzed the physical principles behind the operation of the capacitive plasma probe of the type commonly used for characterization of laser-generated

plasmas. We identified two dominant contributions to the waveforms produced by the probe. The negative contribution to the signal is due to the transient current supplied by the bias voltage source. That contribution is approximately insensitive to the plasma density inside the probe. The positive contribution to the waveform is due to the fraction of free charges, which can be either electrons or ions or both, reaching the charged plates of the probe. The peak value of that contribution is representative of the density of plasma inside the plasma channel. By a simple modification, the probe can be used to measure the mobilities of ions generated through laser excitation, if the nature of the generated ions is known. Using femtosecond plasma excitation in a composite gas allows for the selective measurement of mobilities of ionic species that result from the excitation of the constituent with the lowest ionization potential.

This work was supported by The United States Air Force Office of Scientific Research (US AFOSR) under programs FA9550-10-1-0237 and FA9550-10-1-0561.

¹*Principles of Laser Plasmas*, edited by G. Bekefi (Wiley, New York, 1976).

²A. Couairon and A. Mysyrowicz, *Phys. Rep.* **441**, 47 (2007).

³L. Berge, S. Skupin, R. Nuter, J. Kasparian, and J.-P. Wolf, *Rep. Prog. Phys.* **70**, 1633 (2007).

⁴S. L. Chin, *Femtosecond Laser Filamentation* (Springer, New York, 2010).

⁵M. N. Shneider, A. N. Zheltikov, and R. B. Miles, *Phys. Plasmas* **18**, 063509 (2011).

⁶P. Sprangle, J. Peñano, B. Hafizi, D. Gordon, and M. Scully, *Appl. Phys. Lett.* **98**, 211102 (2011).

⁷P. Polynkin and J. V. Moloney, *Appl. Phys. Lett.* **99**, 151103 (2011).

⁸J. Bernhardt, W. Liu, F. Theberge, H. L. Xu, J. F. Daigle, M. Chateaufneuf, J. Dubois, and S. L. Chin, *Opt. Commun.* **281**, 1268 (2008).

⁹Y.-H. Chen, S. Varma, T. M. Antonsen, and H. M. Milchberg, *Phys. Rev. Lett.* **105**, 215005 (2010).

¹⁰R. G. Meyerand and A. F. Haught, *Phys. Rev. Lett.* **11**, 401 (1963).

¹¹P. Polynkin, M. Kolesik, A. Roberts, D. Faccio, P. Di Trapani, and J. Moloney, *Opt. Express* **16**, 15733 (2008).

¹²S. Akturk, B. Zhou, M. Franco, A. Couairon, and A. Mysyrowicz, *Opt. Commun.* **282**, 129 (2009).

¹³S. Henin, Y. Petit, D. Kiselev, J. Kasparian, and J.-P. Wolf, *Appl. Phys. Lett.* **95**, 091107 (2009).

¹⁴D. Abdollahpour, S. Suntsov, D. G. Papazoglou, and S. Tzortzakis, *Opt. Express* **19**, 16866 (2011).

¹⁵J. L. Pack and A. V. Phelps, *Phys. Rev.* **121**, 798 (1961).

¹⁶E. A. Mason and E. W. McDaniel, *Transport Properties of Ions in Gases* (Wiley, New York, 1988).